

Simultaneous Frequency Transfer and Time Synchronization over a Cascaded Fiber Link of 230 km

Liu Qin¹ Chen Wei² Xu Dan² Cheng Nan² Yang Fei² Gui Youzhen^{1*}
Cai Haiwen² Han Shensheng¹

¹Key Laboratory for Quantum Optics, Shanghai Institute of Optics and Fine Mechanics, Chinese Academy of Sciences, Shanghai 201800, China

²Shanghai Key Laboratory of All Solid-State Laser and Applied Techniques, Shanghai Institute of Optics and Fine Mechanics, Chinese Academy of Sciences, Shanghai 201800, China

Abstract The joint transfer of frequency and one pulse-per-second time signals based on dense wavelength division multiplexing technology is demonstrated over a compensated cascaded fiber link of 230 km, consisting of two stages of fiber links with lengths of 150 km and 80 km. A bi-directional erbium-doped fiber amplifier is inserted in the center of 150 km fiber link to compensate for significant optical attenuation. After every stage has achieved the steady state by optical compensation, the Allan deviation of frequency signal of the cascaded system is 3.1×10^{-14} at 1 s and 6.3×10^{-18} at 10^4 s respectively; the time deviation of time signal is less than 3.5 ps at an averaging time of 10^2 s to 10^4 s. Further, it is verified that the stability of the cascaded link is the standard deviation of the stabilities of the two stages links for both frequency and time signals. After calibration, time synchronization is also realized and the accuracy is within 90 ps.

Key words optical communications; frequency transfer; time transfer; time synchronization; cascaded fiber link; optical compensation

OCIS codes 060.2360; 060.2340; 120.7000

采用级联方式在230 km 光纤链路中同时实现 频率传递和时间同步

刘 琴¹ 陈 炜² 徐 丹² 程 楠² 杨 飞² 桂有珍¹ 蔡海文² 韩申生^{1*}

¹中国科学院上海光学精密机械研究所中科院量子光学重点实验室, 上海 201800

²中国科学院上海光学精密机械研究所上海市全固态激光器与应用技术重点实验室, 上海 201800

摘要 基于波分复用技术,通过级联方式在230 km 光纤链路中实现了频率和时间的同传。该级联系统包含了150 km 和80 km 两级链路系统,其中为了补偿150 km 光纤链路中的损耗,在链路中间放置了一个双向掺铒光纤放大器。当每一级传递系统通过光学补偿方式达到稳定后,整个级联系统的频率稳定度为 3.1×10^{-14} (平均时间1 s时)和 6.3×10^{-18} (平均时间 10^4 s时),时间稳定度为3.5 ps(平均时间 $10^2 \sim 10^4$ s时)。实验结果也证明,不管是对频率信号还是时间信号,都满足误差理论,整个系统的稳定度几乎等于两级链路稳定度的标准偏差。同时通过两级系统的校准,最后得到整个级联系统的时间同步准确度为90 ps。

关键词 光通信; 频率传递; 时间传递; 时间同步; 级联光纤链路; 光学补偿

中图分类号 0439 文献标识码 A

doi: 10.3788/CJL201643.0305006

收稿日期: 2015-10-13; 收到修改稿日期: 2015-11-14

基金项目: 国家自然科学基金(61405227)

作者简介: 刘 琴(1988—),女,博士研究生,主要从事光纤时频传递方面的研究。E-mail: diudiudashu@163.com

导师简介: 韩申生(1960—),男,博士,研究员,博士生导师,主要从事极高能量密度介质中的强非线性过程及其应用、X光相位成像技术、量子成像及光纤时频传递等方面的研究。E-mail: sshan@mail.shcnc.ac.cn

*通信联系人。E-mail: yzgui@siom.ac.cn

1 Introduction

Remote transfer of ultra-stable frequency and time standards is of great importance in many fields such as time measurement, communications, and astronomy. Because of rapid developments in the stabilities of the frequency and time standards^[1-2], especially that of optical clocks^[3-4], the traditional methods based on satellites may no longer satisfy the high stability requirements^[5-6]. Of late, using optical fiber links to realize such a transfer has been considered a promising approach that delivers a much better performance^[7-9].

However, when the total loss along the fiber link is large enough such that the photodetector in the remote end cannot detect the signal, signal regeneration must be considered. Signal regeneration includes two aspects: one is direct optical regeneration and the other is repeater station. Owing to its direct optical amplification, the bi-directional erbium-doped fiber amplifier (Bi-EDFA) has been widely applied in long-distance frequency and time transfer^[10-11]. On the other hand, the transferred distance imposes an ultimate limitation on the feedback bandwidth based on the round-trip compensation method. Therefore, a series of multiplexed Bi-EDFAs connected along the fiber link to realize a long-distance transmission are not suitable for high noise-cancellation bandwidths. A repeater station would be necessary and some experiments on cascaded systems have been carried out to obtain good performances both in the microwave frequencies and in optical frequency transfer^[12-13]. However, in many areas such as long baseline interferometry and deep space networks, time synchronization is also a basic requirement^[14-15]. Consequently, based on the dense wavelength division multiplexing (DWDM) technology, along with transfer of frequency, the transfer of a time signal simultaneously over a compensated cascaded fiber link 230 km in length and time synchronization have also been demonstrated. Relative stabilities of 3.1×10^{-14} at 1 s and 6.3×10^{-18} at 10^4 s for frequency signal have been obtained. A time stability of less than 3.5 ps for an averaging time of 10^2 s to 10^4 s and a time synchronization precision of 90 ps have also been achieved. In addition, apart from frequency signal, time signal also agrees in qualitative with the theory that the stability of the cascaded link is the standard deviation of the stabilities of the two stages. The precision of time synchronization of the cascaded system is almost the sum of these two stages.

Structure of the cascaded system consisting of two stages and the use of an optical compensation method to realize a joint transfer of frequency and time as well as time synchronization between two locations 230 km in distance are described. The detailed principles of phase noise compensation and time synchronization are demonstrated. The experimental results of frequency and time signal stabilities of the two stages and the cascaded system are presented by calculating phase drift and time delay variation, whilst the time synchronization performance is also shown by comparing the absolute time delay between different locations. Finally, the relative result analysis is discussed in detail.

2 Structure of the cascaded system

The schematic diagram of the cascaded system for the joint transfer of frequency and one pulse-per-second (1 PPS) time signal is shown in Fig.1. The local and the remote ends are connected by a repeater station and two fiber links with lengths of 150 km and 80 km, and losses of 38 dB and 18 dB, respectively. A Bi-EDFA is inserted in the center of the 150 km link for compensating significant fiber loss. The cascaded transfer system contains two stages. Stage 1 and stage 2 are similar except that in the fiber link of stage 2 there is no Bi-EDFA, therefore, only stage 1 is described in detail. The experimental temperature is around $23 \text{ }^\circ\text{C} \pm 1 \text{ }^\circ\text{C}$ without air conditioning.

In the local end, a 10 MHz frequency signal from a high-precision clock is multiplied to a higher frequency (1 GHz), because the distributed feedback (DFB) laser generally has a lower intensity of noise at higher frequency levels which results in a higher signal-to-noise rate for the transfer. The 1 PPS time signal is also locked by the same clock. The 1 GHz frequency and the 1 PPS time signals are intensity-modulated on two independent transmitter modules with different wavelengths ($\lambda_1=1548.59 \text{ nm}$ and $\lambda_2=1549.33 \text{ nm}$), each of which contains an electro-optic modulator (EOM) and a DFB laser. In particular, for the 1 PPS signal, the bias point of the EOM is stabilized by a bias controller^[16]. DWDM

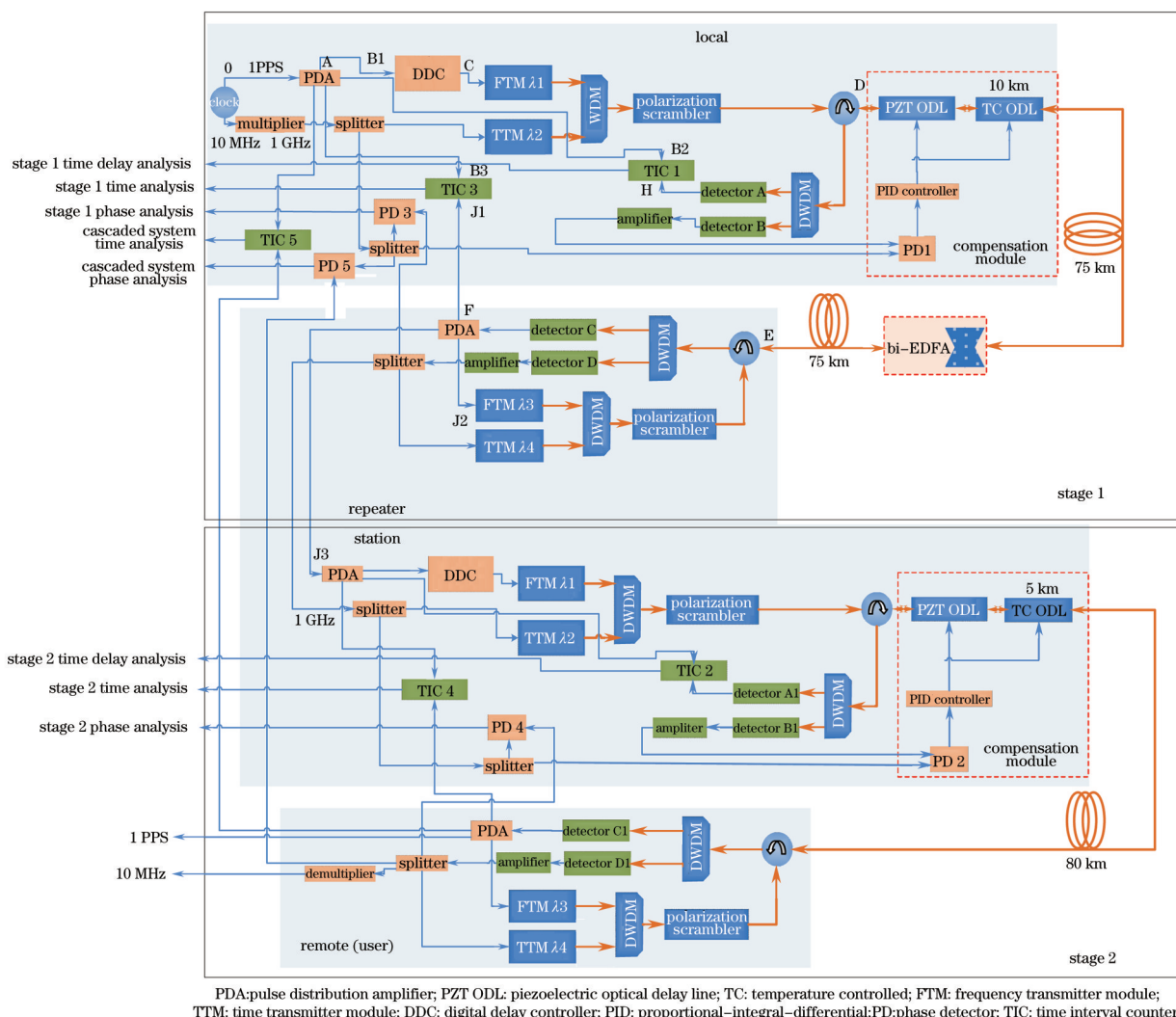


Fig.1 Experimental setup of the cascaded system for a joint 1 GHz transfer of frequency and one PPS time signal

technology has been adopted to multiplex the 1 GHz frequency signal and the 1 PPS time signal. After passing through a polarization scrambler and a circulator, the two carriers enter the fiber link. The polarization scrambler decreases the polarization mode dispersion influence. To compensate the loss in the 150 km fiber, a Bi-EDFA is inserted in the center of the link. In the repeater station, the frequency and time signals demultiplexed by DWDM are detected by two separate low noise photodetectors. The recovered frequency and time signals are divided into three branches. One is used as reference for the next stage and the other is used for signal analysis. Without effective phase-noise cancellation, the stability of the transmitted signals will degrade owing to the phase-noise accumulated along the fiber link. Therefore, the basic concept of the compensation method in fiber frequency and time transfer is the round-trip method^[17]. Hence, the other branches are modulated on two other carriers ($\lambda_3=1547.70$ nm, $\lambda_4=1550.13$ nm) and through the same process as forward transfer, the frequency and time signals reappear in the local end by backward transfer. In the local end, a phase-noise compensation module, including a phase discriminator (PD), a proportional-integral-differential (PID) circuit and a controlled optical delay line (ODL), is applied. The ODL contains a piezoelectric (PZT) ODL and a temperature controlled (TC) ODL. The PZT ODL is a fast fiber stretcher with a bandwidth of 2.2 kHz and a range of 17 ps for the compensation of fast and small variations. The TC ODL has a bandwidth of 10 Hz and ranges of 9.5 ns (5 km) and 16.1 ns (10 km) for the compensation of slow and large fluctuations. For a 1 GHz frequency signal, the returned frequency and reference frequency are sent to the PD 1 to obtain phase noise, and than is processed by the PID circuit to control the PZT ODL and TC ODL. Finally, the fluctuation noise is compensated along the fiber.

3 Methods of frequency compensation and time synchronization

Details of the frequency compensation: the 1 GHz reference signal is set as $V_0 = \cos(\omega t + \varphi_0)$ without considering its amplitude. At the repeater station, it changes to $V_1 = \cos(\omega t + \varphi_0 + \varphi_{ODL} + \varphi_L + \Delta\varphi_p)$, where φ_{ODL} and φ_L are the inherent phase shifts of the ODL and the fiber link considered as constant values, while the one trip phase fluctuation $\Delta\varphi_p$ is the variation term caused by temperature, stress, etc. With a round trip, the signal is detected in the local end and it can be expressed as $V_2 = \cos(\omega t + \varphi_0 + 2\varphi_L + 2\varphi_{ODL} + 2\Delta\varphi_p)$. Both the local reference and the transferred frequency are sent to PD 1, hence, the beat note signal that is proportional to $\varphi_L + \varphi_{ODL} + \Delta\varphi_p$ is obtained. After the PID circuit processing, the error signal $-\Delta\varphi_p$ is sent as feedback to the ODL and the phase of the ODL is changed to $\varphi'_{ODL} = \varphi_{ODL} - \Delta\varphi_p$. Then the signal in the repeater station is stabilized to $V_1 = \cos(\omega t + \varphi_0 + \varphi_{ODL} + \varphi_L)$. The phase difference between the local reference and the transferred frequency in the repeater station is recorded by PD 3. It reflects the stability of stage 1.

As the 1 PPS time signal goes through the same fiber link along with the frequency signal, the influence of the variation caused by temperature and humidity on the fiber is almost the same for both the signals. So the phase noise of the 1 PPS signal is compensated at the same time along with the frequency signal. The time interval counter (TIC) 3 records the difference in the delay between the local 1 PPS signal and the received 1 PPS signal in the repeater station to obtain the stability of the time signal. As the fiber link is compensated, time synchronization can also be obtained^[18-19]. The method is shown in Fig.1. In the first step, without the 150 km fiber link and the Bi-EDFA, the controlled delay time is set as T_1 by the digital delay controller to realize a time synchronization between the local end and the repeater station that is recorded by TIC 3. Thus, $T_{OA} + T_{AB_1} + T_1 + T_{CD} + T_{EF} + T_{FJ_1} - (T_{OA} + T_{AB_3}) = 1$ is obtained. The cables of equal length are selected to make $T_{AB_1} = T_{AB_2} = T_{AB_3}$ and $T_{FJ_1} = T_{FJ_2} = T_{FJ_3}$. At the same time, in the local end, TIC 1 records the delay time T_2 between the reference and the returned signal. Then, $T_{OA} + T_{AB_1} + T_1 + T_{CD} + T_{EF} + T_{FJ_2} + T_{J_2E} + T_{DB_2} - (T_{OA} + T_{AB_2}) = T_2$ is obtained. In the second step, with the 150 km fiber link and the Bi-EDFA, the delay time of the digital delay controller is still set as T_1 , while the value of TIC 1 is T_2' . Then, $T_2 + 2T_{DE} = T_2'$ (i.e., $T_{DE} = \frac{T_2' - T_2}{2}$) is obtained; here it can be assumed that $T_{DE} = T_{ED}$. Next, the delay time of the digital delay controller is reset as T_1' to realize the time synchronization, then $T_{OA} + T_{AB_1} + T_1' + T_{CD} + T_{DE} + T_{EF} + T_{FJ_1} - (T_{OA} + T_{AB_3}) = 1$. Combining with the former equation, the final value of the digital delay controller should be set as $T_1 - \frac{T_2' - T_2}{2}$. However, all the above equations only realize time synchronization between B1 and J1 points. J1 (or J3) point is the real end for the user, but it is O and not the B1 point that is the clock output. Therefore, the time delay T_{OB_1} must be adjusted for synchronization. Then, the time synchronization value changes to $T_1 - \frac{T_2' - T_2}{2} - T_{OB_1}$. In fact, there are two effects that should also be considered and pre-calibrated, which will make the propagation delay time of the two directions different, resulting in $T_{DE} \neq T_{ED}$. One is the wavelength with a 0.8 nm spacing between the back and forth light and the other is asymmetry of the Bi-EDFA^[20]. Using a dispersion analysis machine (MTS-8000-ODM, JDSU), the chromatic dispersion of the 150 km and 80 km fiber spools is measured. The discrimination of delay time is 2508.1 ps/nm and 1335.4 ps/nm, respectively. Then the propagation delay time difference caused by the dispersion is 2.232 ns and 1.188 ns for stage 1 and stage 2, respectively. Besides, for stage 1, the delay time difference caused by the Bi-EDFA is -1.750 ns^[21]. Finally, for stage 1, the time synchronization value is $T_1 - \frac{T_2' - T_2}{2} - T_{OB_1} - 0.48$, and for stage 2, the relative value is $T_1 - \frac{T_2' - T_2}{2} - T_{OB_1} - 1.188$. Then, the digital delay controller can feed forward to compensate the propagation delay and synchronize the 1 PPS time signal of the local end and the repeater station.

Stage 2 exploits the same method to compensate the fiber link and realize the joint transfer of the 1 GHz frequency

and the 1 PPS time signals as well as for the time synchronization. For users, the frequency needs to be down-converted to 10 MHz by a phase-locking module. The values recorded by PD 4 and TIC 4 represent the stability of frequency and time signals of stage 2, respectively. After the two stages have reached a stable state, the properties of the cascaded transfer system can be obtained by the phase difference between the local reference and the transferred frequency in the remote end (recorded by PD 5), and the time delay difference between the local 1 PPS and the received 1 PPS time signals in the remote end (recorded by TIC 5). The bandwidths of all the PDs are 5 Hz. The bandwidths of the detectors for time and frequency are 125 MHz and 1 GHz, respectively, and the sensitivity is 1.05 A/W and 1.00 A/W, respectively. All TICs are Stanford SR620 and the sample interval is 1 s.

4 Experimental results

The results of the overlapping Allan deviation (ADEV) of the frequency calculated from the real-time phase difference recorded by PD 3, PD 4, and PD 5 are shown in Fig.2. The whole testing takes 8.75 h. The open-loop results are obtained by stopping the PZT ODL and the TC ODL, in other words, without optical compensation, the closed-loop results are opposite. The short-term instabilities of 150 km, 80 km, and the cascaded link can reach 2.3×10^{-14} , 1.9×10^{-14} , and 3.1×10^{-14} at 1 s, respectively, whereas the long-term instabilities are 5.1×10^{-18} , 3.5×10^{-18} , and 6.3×10^{-18} at 10^4 s. It can be seen that compared to the open-loop case, the phase-noise in the closed-loop is effectively suppressed. Through the cascaded system, the frequency signal received in the remote end is successfully duplicated from the original reference in the local end, implying that the cascaded system maintains the coherence of the transferred frequency and the reference successfully. As seen from Fig.2, the stability of the cascaded system is almost the standard deviation of the stabilities of stage 1 and stage 2 that can be verified by the error theory. When a system exists with multiple random errors, the total error can be expressed as^[21]

$$\sigma^2 = \sum_{i=1}^n a_i^2 \sigma_i^2 + \sum_{1 \leq i < j} a_i a_j \rho_{ij} \sigma_i \sigma_j, \quad (1)$$

where a_i is the error transfer coefficient and ρ_{ij} is the correlation coefficient between different errors. Since the time-varying propagation delay errors of the two stages are irregular and independent, the noises of each stage are random phase errors and are independent of each other, hence, the values of a_i and ρ_{ij} can be set as 1 and 0, respectively. Then Eq. 1 changes to

$$\sigma^2 = \sum_{i=1}^n \sigma_i^2. \quad (2)$$

Hence, the total propagation delay error of the cascaded link is the standard deviation of the errors of the two stages.

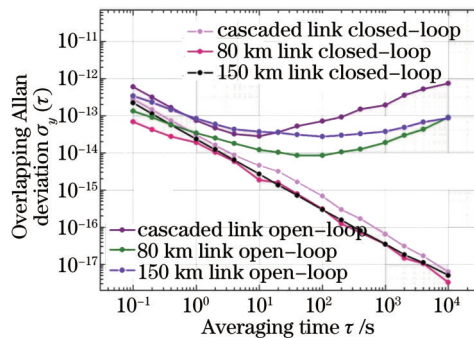


Fig.2 Transferred frequency stabilities of the open-loop and the closed-loop of 150 km, 80 km, and the cascaded link

The stabilities of the transferred time signal denoted by the time deviation (TDEV), calculated from the real-time delay difference recorded by TIC 3, TIC 4, and TIC 5, can be observed in Fig.3. It can be found that the values of 150 km, 80 km and the cascaded closed-loop links decrease to only around 2.9, 1.7, 3.5 ps respectively at an averaging time of 10^2 s to 10^4 s, while in the open-loop link, the values increase sharply verifying that the optical compensation method

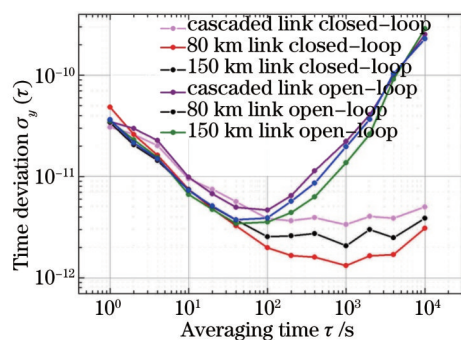


Fig.3 Transferred time stabilities of the open-loop and closed-loop of 150 km, 80 km, and the cascaded link

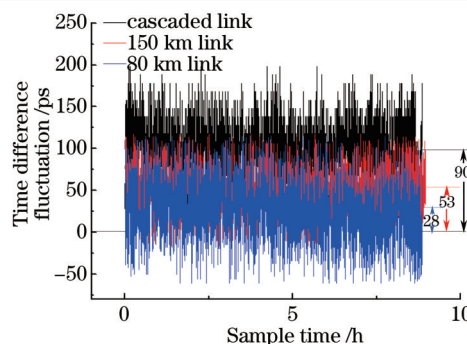


Fig.4 Time synchronization precision of 150 km, 80 km, and the cascaded link

is effective in long-term phase-noise suppression. For the time signal, the stability of the cascaded system is almost the standard deviation of the stabilities of 150 km stage and 80 km stage. The performance of the time synchronization is illustrated in Fig.4. The time synchronization accuracy of 150, 80, 230 km cascaded links is within 53, 28, 90 ps, respectively. The time difference of the cascaded link is slightly larger than the sum of that of 150 km and 80 km links that may be due to some measurement inaccuracy in the TIC.

Relative to the transfer via satellites, all the results show better performance and can meet the high stability requirements of most of the atomic clocks as well as the high time synchronization demands. Therefore, the cascaded system is quite suitable for the ultra-long fiber link transfer of atomic clock signals and for time synchronization.

5 Conclusion

A system disseminating microwave signals through a compensated cascaded fiber link of 230 km with two stages is demonstrated. Based on DWDM technology, time transmission and synchronization are also realized. By an optical compensation method, the fluctuations in the propagation delay of each stage are cancelled out and the entire cascaded transfer system reaches a stable state. The final frequency stability of the cascaded fiber link is improved to 3.1×10^{-14} at 1 s and 6.3×10^{-18} at 10^4 s. The final time stability of the cascaded fiber link is improved to around 3.5 ps at 10^2 s to 10^4 s. It is verified for both frequency and time signals that the stability of the cascaded link is the standard deviation of the stabilities of the two stages. At the same time, by feeding forward to compensate the propagation delay of the 1 PPS time signal of each stage, the time synchronization between the local end and the remote end through the cascade fiber link is also achieved. The accuracy of time synchronization is 90 ps. At such performance, it can be foreseen that with more stages, the transferred distance can extend to thousands of kilometers and it can still satisfy most of the practical time and frequency applications at present.

References

- 1 R Li, K Gibble, K Szymaniec. Improved accuracy of the NPL-CsF₂ primary frequency standard: Evaluation of distributed cavity phase and microwave lensing frequency shifts[J]. Metrologia, 2011, 48(5): 283-289.
- 2 S Weyers, V Gerginov, N Nemitz, *et al.*. Distributed cavity phase frequency shifts of the caesium fountain PTB-CsF₂[J]. Metrologia, 2012, 49(1): 82-87.
- 3 I Ushijima, M Takamoto, M Das, *et al.*. Cryogenic optical lattice clocks[J]. Nat Photon, 2015, 9(3): 85-189.
- 4 B J Bloom, T I Nicholson, J R Williams, *et al.*. An optical lattice clock with accuracy and stability at the 10^{-18} level[J]. Nature, 2014, 506(6): 71-75.
- 5 D Piester, A Bauch, L Breakiron, *et al.*. Time transfer with nanosecond accuracy for the realization of international atomic time[J]. Metrologia, 2008, 45(2): 185-198.
- 6 W Tseng, S Lin, K Feng, *et al.*. Improving TWSTFT short-term stability by network time transfer[J]. IEEE Trans Ultrason, Ferroelectr, Freq Control, 2010, 57(1): 161-167.
- 7 O Lopez, A Amy-Klein, C Daussy, *et al.*. 86-km optical link with a resolution of 2×10^{-18} for RF frequency transfer[J]. Eur Phys J D, 2008,

- 48(1): 35–41.
- 8 O Lopez, A Haboucha, B Chanteau, *et al.*. Ultra-stable long distance optical frequency distribution using the Internet fiber network[J]. *Opt Express*, 2012, 20(21): 23518–23526.
- 9 S Droste, F Ozimek, T Udem, *et al.*. Optical-frequency transfer over a single-span 1840 km fiber link[J]. *Phys Rev Lett*, 2013, 111(11): 110801.
- 10 M Amemiya, M Imae, Y Fujii, *et al.*. Precise frequency comparison system using bidirectional optical amplifiers[J]. *IEEE Trans Instrum Meas*, 2010, 59(3): 632–640.
- 11 Ł Sliwczynski, P Krehlik, Ł Buczek, *et al.*. Frequency transfer in electronically stabilized fiber optic link exploiting bidirectional optical amplifiers[J]. *IEEE Trans Instrum Meas*, 2012, 61(9): 2573–2580.
- 12 M Fujieda, M Kumagai, S Nagano. Coherent microwave transfer over a 204-km telecom fiber link by a cascaded system[J]. *IEEE Trans Ultrason, Ferroelect, Freq Contr*, 2010, 57(1): 168–174.
- 13 O Lopez, A Haboucha, F Kefelian, *et al.*. Cascaded multiplexed optical link on a telecommunication network for frequency dissemination [J]. *Opt Express*, 2010, 18(16): 16849–16857.
- 14 D S Robertson. Geophysical applications of very-long-baseline interferometry[J]. *Rev Mod Phys*, 1991, 63(4): 899–918.
- 15 M Calhoun, S Huang, R L Tijoelker. Stable photonic link for frequency and time transfer in the deep-space network and antenna arrays [C]. *Proc IEEE*, 2007, 95(10): 1931–1946.
- 16 Cheng Nan, Chen Wei, Liu Qin, *et al.*. Bias point control system of electro-optic modulator used for transferring one pulse per second [J]. *Chinese J Lasers*, 2015, 42(9): 0905002.
程楠, 陈伟, 刘琴, 等. 应用于秒脉冲传递的电光调制器反馈控制系统[J]. *中国激光*, 2015, 42(9): 0905002.
- 17 S M Foreman, K W Holman, D D Hudson, *et al.*. Remote transfer of ultrastable frequency references via fiber networks[J]. *Rev Sci Instrum*, 2007, 78(2): 021101.
- 18 P Krehlik, Ł Sliwczynski, Łukasz Buczek, *et al.*. Fiber-optic joint time and frequency transfer with active stabilization of the propagation delay[J]. *IEEE T Instrum Meas*, 2012, 61(10): 2844–2851.
- 19 Cheng Nan, Chen Wei, Liu Qin, *et al.*. Time synchronization technique for joint time and frequency transfer via optical fiber[J]. *Chinese J Lasers*, 2015, 42(7): 0705002.
程楠, 陈伟, 刘琴, 等. 光纤时间频率同时传递系统中时间同步方法的研究[J]. *中国激光*, 2015, 42(7): 0705002.
- 20 Wei Chen, Qin Liu, Nan Cheng, *et al.*. Joint time and frequency dissemination network over delay-stabilized fiber optic links[J]. *Photonics J*, 2015, 7(3): 7901609.
- 21 Qin Liu, Wei Chen, Dan Xu, *et al.*. Bi-directional erbium-doped fiber amplifiers used in joint frequency and time transfer based on WDM technology[J]. *Chin Opt Lett*, 2015, 13(11): 110601.
- 22 Y T Fei. *Error Theory and Data Processing*[M]. 5th ed, Beijing: Machinery Industry Press, 2004: 176–177.

栏目编辑: 王晓琰